Two Enzymes with a Common Function but Different Heme Ligands in the Forms as Isolated. Optical and Magnetic Properties of the Heme Groups in the Oxidized Forms of Nitrite Reductase, Cytochrome cd_1, from *Pseudomonas stutzeri* and *Thiosphaera pantotropha*†

Myles R. Cheesman,*,‡ Stuart J. Ferguson,§ James W. B. Moir,|| David J. Richardson,⊥ Walter G. Zumft,# and Andrew J. Thomson‡

Centre for Metalloprotein Spectroscopy and Biology, School of Chemical Sciences, University of East Anglia, Norwich NR4 7TJ, U.K., Centre for Metalloprotein Spectroscopy and Biology, School of Biological Sciences, University of East Anglia, Norwich NR4 7TJ, U.K., Department of Biochemistry, University of Oxford, Oxford OX1 3QU, U.K., The Krebs Institute, Department of Molecular Biology and Biotechnology, University of Sheffield, Sheffield S10 2UH, U.K., and Lehrstuhl für Mikrobiologie, Universität Fridericiana, D-76128 Karlsruhe, Germany

Received July 10, 1997; Revised Manuscript Received October 1, 1997⊗

ABSTRACT: It is shown that, in the oxidized state, heme *c* of *Pseudomonas stutzeri* (ZoBell strain) cytochrome cd_1 has histidine-methionine ligation as observed for cytochrome cd_1 from *Pseudomonas aeruginosa* [Sutherland, J., Greenwood, C., Peterson, J., and Thomson, A. J. (1986) *Biochem. J. 233*, 893−898]. However, the X-ray structure of *Thiosphaera pantotropha* cytochrome cd_1 reveals bis-histidine ligation for heme *c*. It is confirmed by EPR and near-infrared (NIR) MCD measurements that the bis-histidine coordination remains unaltered in the solution phase. Hence, the difference between the heme *c* ligation states defines two distinct classes of oxidized cytochromes cd_1 as isolated. A weak feature in the *T. pantotropha* NIR MCD at 1900 nm suggests that a small population of heme *c* has histidine-methionine coordination. The ligation state of heme d_1 cannot be defined with the same level of confidence, because the porphyrin-to-Fe(III) charge-transfer (CT) bands are less well characterized for this class of partially reduced porphyrin ring. However, variable temperature absorption and MCD spectra show that, in the *T. pantotropha* enzyme, heme d_1 exists in a thermal low-spin/high-spin mixture with the low-spin as the ground state, whereas in *P. stutzeri* cytochrome cd_1, and d_1 heme is low-spin at all temperatures. A weak band, assigned as the heme d_1 porphyrin-$\pi(a_{1u},a_{2u})$-to-ferric(d) charge-transfer transition has been identified for the first time at 2170 nm. Its magnetic properties show the heme d_1 to have an unusual $(d_{xz,yz})^4(d_{xy})^1$ electronic ground state as is found for low-spin Fe(III) chlorins [Cheesman, M. R., and Walker, F. A. (1996) *J. Am. Chem. Soc. 118*, 7373−7380]. It is proposed that the localization of the Fe(III) unpaired d-electron in an orbital lying in the heme plane may decrease the affinity of the Fe(III) heme for unsaturated ligands such as NO. Although heme d_1 in the enzymes from *P. stutzeri* and *T. pantotropha* shows different temperature-dependent spin properties, the positions of the low-spin Fe(III) α-absorption band, at ∼640 nm, are very similar to those observed for cytochromes cd_1 from eight other sources, suggesting that all have similar strength fields from the axial ligands and, hence, that all have the same coordination, namely histidine-tyrosine or possibly histidine-hydroxide at the heme.

In bacterial denitrification, nitrate is reduced to dinitrogen gas *via* three intermediates, nitrite, nitric oxide, and nitrous oxide (*1*−*3*). The second step in this process, the one-electron reduction of nitrite to nitric oxide ($2H^+ + e^- + NO_2^- \rightarrow NO + H_2O$) is catalyzed, in any particular denitrifier, by one of two distinct respiratory-type nitrite reductases. One is a copper enzyme containing both type I and type II centers (*4*, *5*). The other enzyme, cytochrome cd_1 (cd_1),[1] is a homodimeric water-soluble periplasmic protein containing two heme groups per monomer. One heme, a c-type, is bound *via* a Cys-X-X-Cys-His motif. The second heme, noncovalently bound and known as heme d_1, is a ferric-dioxoisobacteriochlorin cofactor unique to this class of enzyme, (*6*, *7*). Heme d_1 appears to be the site of nitrite reduction while heme *c* functions to transfer electrons to heme d_1 from an external electron donor, either a c-type cytochrome or a cupredoxin (*8*). Curiously, cytochrome cd_1 also has oxidase activity. Indeed, *P. aeruginosa* enzyme was originally described as a cytochrome *c* oxidase (*9*).

† This work was supported by grants from BBSRC BO3032-1 (A.J.T. and D.J.R.), BBSRC BO5860 and EC Biotech. BIO4-CT96-0281 (S.J.F.) and by the Deutsche Forschungsgemeinschaft and Fonds der Chemischen Industrie (W.G.Z.).

* Address correspondence to this author at the School of Chemical Sciences, University of East Anglia, Norwich, NR4 7TJ, United Kingdom. Telephone: +44 (1603) 592028. Fax: +44 (1603) 592710. E-mail: m.cheesman@uea.ac.uk.

‡ School of Chemical Sciences, University of East Anglia.

§ University of Oxford.

|| University of Sheffield.

⊥ School of Biological Sciences, University of East Anglia.

Universität Fridericiana.

⊗ Abstract published in *Advance ACS Abstracts,* December 15, 1997.

[1] Abbreviations: cd_1, cytochrome cd_1; *P. stutzeri*, *Pseudomonas stutzeri*; *T. pantotropha*, *Thiosphaera pantotropha*; *T. denitrificans*, *Thiobacillus denitrificans*; *R. eutropha*, *Ralstonia eutropha*; *P. denitrificans*, *Paracoccus denitrificans*; *P. aeruginosa*, *Pseudomonas aeruginosa*; EPR, electron paramagnetic resonance; MCD, magnetic circular dichroism; NIR-CT, near-infrared charge-transfer; RT, room temperature.

S0006-2960(97)01677-2 CCC: $14.00

```
          1         11   H17(c)21 Y25(d)  31         41         50
T.pantotropha QEQVAPPKDP AAALEDHKTR TDNRYEPSLD NLAQQDVAAP GAPEGVTALS
P.aeruginosa -------KDD MKAAEQYQG- AASAVDP--- ---AHVVRTN GAPD----MS
P.stutzeri ZB ---------- ---------- ---------- ----LAVAQA AAPE----MT
P.stutzeri JM ---------- ---------- ---------- ----MAVAHA AAPD----MT
R.eutropha    ---------- ---LPHAATK AEPKAEP--- ------K--A AIPT----LT
                                                        *

         51         61   H69(c)71         81         91        100
T.pantotropha DAQYNEANKI YFERCAGCHG VLRKGATGKA LTPDLTRDLG ----------
P.aeruginosa  ESEFNEAKQI YFQRCAGCHG VLRKGATGKP LTPDITQQRG ----------
P.stutzeri ZB AEEKEASKQI YFERCAGCHG VLRKGATGKN LEPHWSKTEA DGKKTEGGTL
P.stutzeri JM AEEKEAAKKI YFERCAGCHG VLRKGATGKN LEPHWEKTED -GKKIEGGTL
R.eutropha    AAEFDHARQI YFERCAGCHG VLRKGATGKS LTPDITRARG ----------
                     * ** ******* *********  * *

         101        111    M106121        131  M123  141     →150
T.pantotropha ---FDYLQSF ITYASPAGMP NWGTSGELSA EQVDLMANYL LLDPAAPPEF
P.aeruginosa  ---QQYLEAL ITYGTPLGMP NWGSSGELSK EQITLMAKYI QHTPPQPPEW
P.stutzeri ZB NLGTKRLENI IAYGTEGGMV NY--DDILTK EEINMMARYI QHTPDIPPEF
P.stutzeri JM KLGTKRLENI IAFGTEGGMV NY--DDILTA EEINLMARYI QHTPDIPPEF
R.eutropha    ---TEYLKTF IKYGSPAGMP NWGTSGDLTD PEVDLMARYI QLDPPTPPEY
                    *    *      **  *      *        ** *     *  ***

         151        161        171        181        191       200
T.pantotropha GMKEMRESWK VHVAPEDRPT QQENDWDLEN LFSVTLRDAG QIALIDGTTY
P.aeruginosa  GMPEMRESWK VLVKPEDRPK KQLNDLDLPN LFSVTLRDAG QIALVDGDSK
P.stutzeri ZB SLQDMKDSWN LIVPVEKRVT KQMNKINLQN VFAVTLRDAG KLALIDGDTH
P.stutzeri JM SLQDMKDSWN LIVPVERR-- RQMNKVNLEN VFAITLRDA- -Q-LWDGDTH
R.eutropha    SLADIEKSRK DILPVAQRPT KKMNQYNLDN LFSVTLRDAG EVALIDGDSK
                   *          *      *   * *  *  *****     * **

         201        211H200(d) 221        231        241       250
T.pantotropha EIKSVLDTGY AVHISRLSAS GRYLFVIGRD GKVNMIDLWM KEPTTVAEIK
P.aeruginosa  KIVKVIDTGY AVHISRMSAS GRYLLVIGRD ARIDMIDLWA KEPTKVAEIK
P.stutzeri ZB KIWKVLESGY AVHISRMSAS GRYVYTTGRD GLTTIIDLWP EEPMTVATVR
P.stutzeri JM EIWKILDTGY AVHISRLSAS GRMSTPSAG- WLTTIIDMWY PEPTTVATVR
R.eutropha    QIINIVKTGY AVHISRMSAS GRYLYVIGRD ARLDLIDLWL PKPDIVAEVK
               *      ** ****** *** **              ** *    *  **
```

FIGURE 1: Sequence alignments of the N-terminal amino acid regions of cytochromes cd_1 from *T. pantotropha* (*13*); *P. aeruginosa* (*14*); *P. stutzeri* ZoBell (ZB) (*15*); *P. stutzeri* JM300 (JM) (*16*); *R. eutropha* (*17*). Potential metal ligands and the site of covalent *c*-heme attachment are shown in bold. The ligands for the *c*- and d_1-hemes of oxidized cytochrome cd_1 from *T. pantotropha* as determined from the crystal structure are underlined. These and other important residues are labeled, also according to the *T. pantotropha* sequence. Of particular note is that His-17, which coordinates to *c*-heme of cytochrome cd_1 from *T. pantotropha*, is not conserved in the sequences from *P. aeruginosa* or either *P. stutzeri* strain and that a tyrosine near the N-terminal is found only for *T. pantotropha* (the d_1-heme ligand Tyr-25) and for *P. aeruginosa*. An asterisk indicates a conserved residue, (→) the beginning of the d_1-binding domain.

The substrate reduction product, nitric oxide, normally binds tightly to hemes, especially those in the ferrous state. It is not clear whether nitric oxide release is facilitated by some intrinsic property of heme d_1 itself or by some other mechanism arising from, for example, displacement by a protein ligand to the iron. Involvement of a heme ligand was implicated when the three-dimensional structure of *T. pantotropha* cytochrome cd_1 in the oxidized state was solved to 1.55 Å (*10*, *11*). The structure revealed that each subunit comprises two distinct domains. Heme-*c* is in an α-helical domain (amino acid residues 1−134) and is bound by two histidine residues (His-17 and His-69) while heme d_1 is at the center of an eight-bladed β-propeller structure (residues 135−567). Heme d_1 ligands are His-200 and, unexpectedly, Tyr-25 from the heme *c* binding domain. A mechanism for the enzyme has been proposed, which involves displacement of the tyrosine ligand on reduction allowing nitrite to bind (*11*). As heme d_1 becomes oxidized during reduction of nitrite, tyrosine rebinds ferric heme d_1, thus, displacing the product, nitric oxide. EPR and MCD spectra of the cytochrome cd_1 from *P. aeruginosa* showed that heme d_1 changes from low-spin and high-spin upon reduction, suggesting a change in coordination state (*12*).

Although the crystal structure of *T. pantotropha* oxidized cytochrome cd_1 suggests important roles for specific residues, a comparison of known cytochrome cd_1 primary sequences shows that not all of these residues are conserved (Figure 1). Only one of the two histidine ligands to heme *c* in the *T. pantotropha* enzyme (His-69) is conserved in the sequences of the cytochromes cd_1 from *P. aeruginosa*, *P. stutzeri* (strains ZoBell and JM300), and *Ralstonia* (formerly *Alcaligenes*) *eutropha* (*13*−*17*). This is consistent with earlier MCD spectroscopy showing that the heme *c* of the *P. aeruginosa* enzyme has histidine-methionine ligation (*18*). Similarly, although the heme d_1 histidine ligand (His-200) of *T. pantotropha* is a conserved residue, only *P. aeruginosa* possesses a tyrosine near the N-terminus which might fulfill the role of Tyr-25. It does, however, lack a heme *c* histidine ligand eight residues back toward the N-terminus.

These considerations raise two questions. First, is it the case that cytochrome cd_1, despite being a relatively specialized enzyme, does not have conserved amino acid residues as ligands to its heme centers, and if so, what candidate ligands can be identified for the enzymes from *P. aeruginosa* and *P. stutzeri*? Second, is it possible that the crystal structure of oxidized cytochrome cd_1, from *T. pantotropha* represents a form of the enzyme that is not on the catalytic pathway? In this context, the discovery of tyrosine ligation to heme d_1 is of interest because this residue is known to have a very high affinity for the oxidized form of b-type heme, which means that its redox potential should be shifted below 0 mV. There is, at present, no evidence that ligation of tyrosine to the heme d_1 shifts the redox potential to negative values to the extent that reduction of the enzyme by its physiological donors (with redox potentials in the range 200−300 mV) would become impossible. Nevertheless, confirmation that solution properties of the enzyme are consistent with ligation by this tyrosine residue would be valuable.

The use of MCD spectroscopy to investigate proteins containing b- and c-type hemes is well established. These hemes and other protoporphyrin IX derivatives will be referred to as *protohemes*. The patterns and intensities of the MCD spectra throughout the UV−visible wavelength region allow assignment of the spin and oxidation states of the heme iron (*19*). Ferric heme charge-transfer (CT) bands, of both low- and high-spin forms, lie at longer wavelengths (600−2300 nm) and are readily detected by MCD spectroscopy. The signs and the energies of these transitions provide information concerning spin-state and the identity of the heme ligands (*20*). The optical and MCD spectra of hemes with partially reduced exocyclic rings (*hydroporphyrins*) have, by contrast, been less well characterized, and assignments are less clear. For example, the iron-chlorin, known as heme *d*, occurs as one of three hemes in the quinol-oxidase cytochrome *bd* and as the only prosthetic group in hydroperoxidase II (HPII). Limited MCD data available for these heme *d* systems reveal spectroscopic properties distinct from those of protohemes (*21*−*26*). It is clear that low-spin ferric heme *d* gives rise to CT spectra in the near-infrared (NIR) region of unusually low intensity. In the case of HPII, weak NIR-CT bands have been located (*23*, *25*, *27*), but for cytochrome *bd*, the MCD spectrum at all wavelengths is dominated by the more intense signatures of the b-type hemes (*28*). In *low-spin ferric* protohemes, the intensity of the MCD NIR-CT band depends on, *inter alia*, the rhombicity of the ligand field imposed at the ferric ion by the axial ligands. It had been proposed that the anomalously low NIR MCD intensity for heme *d* is due to high rhombicity resulting from the lower macrocycle symmetry (*23*). But, on the contrary, it has been shown that these MCD properties are due to an unexpected $(d_{xz,}d_{yz})^4(d_{xy})^1$ electronic ground state (*29*). This property also provides an explanation for the unusual but characteristic EPR spectra of low-spin ferric chlorins.

Prompted by these observations, we have undertaken a comparison of the properties of the cytochromes cd_1 from *P. stutzeri* (ZoBell) and *T. pantotropha* using the MCD and EPR techniques which have provided much valuable information concerning the heme properties in the enzyme from *P. aeruginosa*. The results obtained fully support the surprising previous indications that enzymes from different sources are not identical with respect to heme iron ligands in the oxidized state and hence there may be several classes of cytochrome cd_1.

MATERIALS AND METHODS

Purification of Cytochrome cd_1 from Pseudomonas stutzeri (ZoBell). Cytochrome cd_1 from *P. stutzeri* strain ZoBell (ATCC 14405) was purified from anaerobically nitrate-grown cells (*30*). The cell paste was used immediately after harvest and not frozen prior to cell breakage in a high-pressure homogenizer (Rannie). The enzyme was followed during purification by measuring nitrite-reducing activity with ascorbate-reduced phenazine methosulfate as the electron donor system. The purification procedure comprised ion exchange chromatography on DE-52 (Whatman), Sephadex G-100 gel filtration, preparative isoelectric focusing with Ultrodex as support material (Pharmacia) and a final Sephacryl S-200 chromatography step in 50 mM Tris-HCl, pH 7.5. The focusing step was essential to remove various contaminating cytochromes from the enzyme, and to separate cytochrome cd_1 from nitrous oxide reductase (*30*). Cytochrome cd_1 focused around pI $\approx$ 5.2. The enzyme was concentrated by ultrafiltration with a PM10 membrane (Amicon) and stored in liquid nitrogen until use. The enzyme has a molecular mass of 119−134 kDa as judged by gel filtration and nondenaturing gradient electrophoresis. SDS−PAGE shows a subunit size of 60−65 kDa, compared to a sequence-derived M_r of 59 532.

Purification of Cytochrome cd_1 from Thiosphaera pantotropha. Cytochrome cd_1 from *T. pantotropha* was purified using the procedure previously described (*31*). The chromatographic purification of cytochrome cd_1 from periplasmic extracts isolated from anaerobically grown *T. pantotropha* yielded 5 mg of purified protein/L of culture. The protein purity was checked using SDS−PAGE. Protein concentration was measured using the Bradford assay with reagents obtained from Biorad. Samples were concentrated for spectroscopic analysis using Filtron Microsep microconcentrators with a 30 kDa cutoff. Buffer exchange was performed using Sephadex G25-M PD10 columns obtained from Pharmacia.

T. pantotropha is now thought to be a strain virtually identical to *P. denitrificans* and is also designated as *P. denitrificans* strain GB17. In the subsequent discussion, the cytochromes cd_1 from *P. denitrificans* and *T. pantotropha* are assumed to be equivalent. The sequences of the mature proteins are 97% identical (*13*).

Spectroscopic Measurements. The intensities of spectra presented herein are referred to concentrations of cytochrome cd_1 *monomer* and were calculated using the Soret band electronic absorption intensity and assuming extinction coefficients of $\epsilon_{411nm} = 141\ mM^{-1}\ cm^{-1}$ for the *P. stutzeri* enzyme (*18*) and $\epsilon_{406nm} = 148\ mM^{-1}\ cm^{-1}$ for the *T. pantotropha* enzyme (*31*). Samples for spectroscopic examination were prepared in deuterium oxide solutions containing 50 mM HEPES-NaOH, at pH* = 7.5 (*P. stutzeri*) and 50 mM Tricine at pH* = 8.0 (*T. pantotropha*). (pH* is the apparent pH of the D_2O solutions measured using a standard glass pH electrode.)

Electronic absorption spectra were recorded on a Hitachi U-4001 spectrophotometer. Ultra-low-temperature absorption spectra of samples frozen in the MCD cryostat were

measured using the same spectrometer. The cryostat was located in the spectrometer using a modified sample compartment base-plate from Hitachi.

EPR spectra were recorded on an X-band ER-200D spectrometer (Brüker Spectrospin) interfaced to an ESP1600 computer and fitted with a liquid helium flow-cryostat (ESR-9; Oxford Instruments). Magnetic circular dichroism (MCD) spectra were recorded on either a circular dichrograph, JASCO J-500D, for the wavelength range 280−1000 nm or a laboratory-built dichrograph (*20*) for the range 800−2500 nm. Samples were mounted within an Oxford Instruments SM4 split-coil superconducting solenoid capable of generating magnetic fields up to 5 T for low-temperature measurements and in an Oxford Instruments SM1 6 T superconducting solenoid with an ambient-temperature bore for room temperature measurements. To obtain optical quality glasses on freezing for low-temperature MCD measurements, glycerol was added to samples to a level of 50% v/v (*32*). These additions did not significantly alter the EPR or room temperature electronic absorption spectra.

RESULTS

A comparison has been made between the coordination modes and spin states of both heme groups in cd_1 from *P. stutzeri* and *T. pantotropha* at room temperature by means of absorption and MCD spectroscopy and at liquid helium temperatures using electronic absorption, MCD, and EPR spectroscopy.

Ultraviolet and Visible (UVV) Region Electronic Absorption Spectra. The ultraviolet and visible (UVV) region electronic absorption spectra, Figure 2, show obvious differences between the two enzymes. Heme *c* in the *low-spin* ferric state gives rise to transitions between 300 and 600 nm, which are seen, at room temperature, in the Soret region (*P. stutzeri*, 411 nm; *T. pantotropha*, 406 nm) and as the α,β bands between 520 and 560 nm. Heme d_1 will also contribute to the absorption at these wavelengths (*6*, *7*, *33*, *34*). The α-bands of ferric isobacteriochlorins are red-shifted relative to those of heme *c* allowing, at wavelengths longer than 600 nm, the observation of bands due solely to heme d_1. In this region, there is a significant difference between the spectra of the two enzymes. For *P. stutzeri* cd_1, one band is observed at 641 nm with $\epsilon = 18.5$ mM^{-1} cm^{-1}, an intensity similar to that reported for ferric heme d_1 both in other cytochromes cd_1 (*35*, *36*) and in heme d_1-substituted myoglobin (*37*). However, for *T. pantotropha*, two bands of approximately half this intensity are seen at 644 nm and 702 nm (Figure 2c). Absorption spectra measured at lower temperatures show that the *T. pantotropha* enzyme is a mixture of two species in thermal equilibrium rather than a single species with two bands. At 1.75 K, the absorption spectra of the *P. stutzeri* and *T. pantotropha* enzymes are virtually identical with one heme d_1 α-band at ∼644 nm. On raising the temperature of a sample of *T. pantotropha* cd_1, a second band at 702 nm appears, whereas the absorption spectrum of the *P. stutzeri* enzyme is unchanged. As the temperature is further raised, the 644 nm band decreases in intensity and the second band at 702 nm grows, eventually giving at room temperature the spectrum of Figure 2c. No spectra were recorded in the temperature range 180−290 K as a phase change in the buffer/glycerol mixture at ∼200 K renders the sample opaque. A shoulder at ∼430 nm, Figure 2c, appears simultaneously with the 702 nm band, Figure 2d. In the spectrum of the *T. pantotropha* enzyme at room temperature, an additional very weak (ϵ < 800 M^{-1} cm^{-1}) broad band can be detected at ∼1100 nm. Although it is too weak to be followed precisely in the variable temperature spectra, it has no counterpart in the room temperature spectrum of the *P. stutzeri* enzyme. It is therefore concluded that this band is also due to the species giving rise to the 702 nm band. All these observations are consistent with the ferric heme d_1 of *T. pantotropha* cytochrome cd_1 existing as a low-spin/high-spin thermal mixture. Absorption studies on extracted heme d_1 and on the heme d_1·apo-myoglobin complex show that low-spin ferric bands near 640 nm are shifted to the red in high-spin forms (*38*, *39*). Therefore in *P. stutzeri* cytochrome cd_1, heme d_1 is low spin at all temperature, but for the *T. pantotropha* enzyme, this is the ground state and, at room temperature, the high-spin state is also significantly populated.

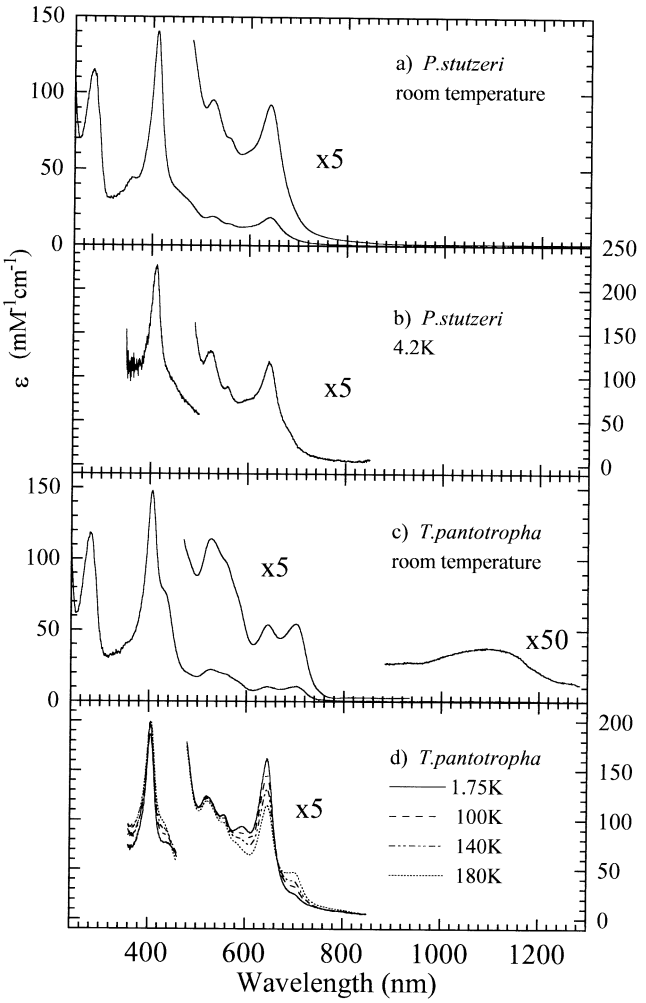

FIGURE 2: Electronc absorption spectra of oxidized cytochromes cd_1. (a) *P. stutzeri* cd_1 at room temperature (91 μM and 1.13 mM); (b) *P. stutzeri* cd_1 at 4.2 K (52 and 545 μM); (c) *T. pantotropha* cd_1 at room temperature (45 and 490 μM); (d) *T. pantotropha* cd_1 at 1.75 K (—); 100 K (− − −); 140 K (− - - −); 180 K (···) (21 and 200 μM). Buffers were as described in Materials and Methods.

Ultraviolet and Visible (UVV) Region MCD Spectra. The UVV MCD spectra of the two enzymes, shown in Figure 3, are strongly temperature dependent, consistent with the paramagnetic nature of the heme chromophores. The RT MCD spectrum of *P. stutzeri* cd_1 between 300 and 580 nm (Figure 3a) is typical of low-spin ferric protoheme (*19*),

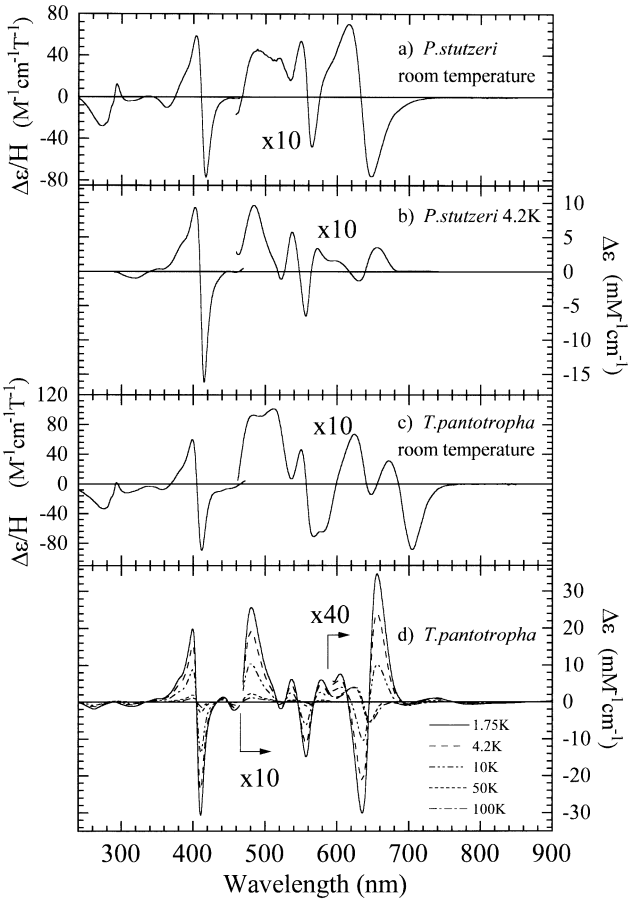

FIGURE 3: Ultraviolet and visible region MCD spectra of oxidized cytochromes cd_1. (a) *P. stutzeri* cd_1 at room temperature (91 and 1.13 μM); (b) *P. stutzeri* cd_1 at 4.2 K (52 and 545 μM); (c) *T. pantotropha* cd_1 at room temperature (45 and 490 μM); (d) *T. pantotropha* cd_1 at 1.75 K (—); 4.2 K (− − −); 10 K (− - − -); 50 K (- - - -); 100 K (− - − -) (21 and 200 μM). Buffers were as described in Materials and Methods.

implying that contributions in this region from low-spin ferric heme d_1 are significantly weaker than those of heme *c*. The intensities of RT MCD spectra of ferric isobacteriochlorins support this view (*33*). The low-temperature MCD spectrum of the *P. stutzeri* enzyme, Figure 3b, is also dominated by heme *c*. The bis-imidazole complex of heme d_1 gives a Soret MCD band at 4.2 K with a peak-to-trough intensity of ~2.5 mM^{-1} cm^{-1} (*34*), an order of magnitude weaker than that of low-spin ferric c-type heme. The 641 nm absorption band of heme d_1 appears in the MCD as a derivative-shaped feature centered near 633 nm. In Figure 3, panels a and b, this derivative shows unusual behavior in that it changes sign between RT and 4.2 K. MCD intensity comprises three types of contribution: *A*, *B*, and *C* terms (*40*, *41*), which arise respectively from degeneracies in the ground and/or excited states, magnetic field induced mixing of states, and population changes across the Zeeman split components of a degenerate ground state. The *C* term is the temperature-dependent term characteristic of paramagnets and usually dominates the MCD at liquid helium temperatures. Strong *A* term contributions of opposite sign in the RT MCD are the likely source of this sign change for the heme d_1 features. The phenomenon is common to the MCD of both enzymes, and the progressive sign change is shown at several temperatures in the spectra of *T. pantotropha* cd_1, Figure 3d. Where the spectrum is dominated by *C* term intensity, the spectra at different temperatures pass through isosbestic

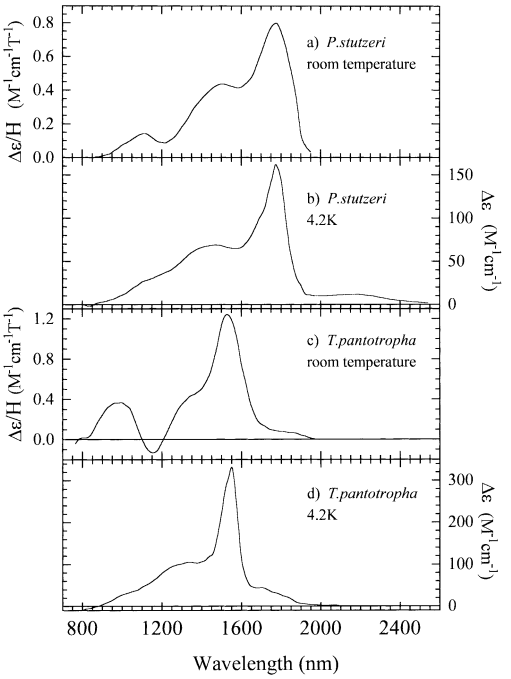

FIGURE 4: Near-infrared region MCD spectra of oxidized cytochromes cd_1. (a) *P. stutzeri* cd_1 at room temperature (1.13 mM); (b) *P. stutzeri* cd_1 at 4.2 K (545 μM); (c) *T. pantotropha* cd_1 at room temperature (490 μM); (d) *T. pantotropha* cd_1 at 4.2 K (200 μM). Buffers were as described in Materials and Methods.

points on the $\Delta\epsilon = 0$ axis. In the 610−690 nm region, this occurs only at temperatures below 10 K. As the *C* term intensity diminishes, the opposite sign *A* term features become the more important contributions. The transition is essentially complete before 50 K. This switch to a different MCD intensity mechanism gives rise to isosbestic points which are *off* the $\Delta\epsilon = 0$ axis at 613 and 644 nm. The derivative is then temperature independent. At these temperatures, MCD bands corresponding to the high-spin ferric heme d_1 absorption at 702 nm have not yet appeared. At RT, Figure 3c, they are seen as a second derivative shaped pair centered near 685 nm. At 4.2 K, where heme d_1 is low-spin in both enzymes, the spectra are similar both to each other and to that of *P. aeruginosa* cd_1 (*12*, *18*).

NIR MCD Spectra. Figure 4 shows the MCD spectra of both enzymes at RT and at 4.2 K in the region 800−2500 nm. The differences between the two enzymes are again striking. The prominent positive peaks at 1775 nm for *P. stutzeri* cd_1 and at 1530 nm in the spectra of *T. pantotropha* cytochrome cd_1, both with a weaker shoulder to higher energy, are the NIR-CT bands expected for low-spin ferric protohemes. The band maximum at 1775 nm lies in the range characteristic of low-spin Fe(III) heme coordinated by methionine and histidine, whereas the band at 1530 nm is characteristic of bis-histidine coordination consistent with the X-ray determined structure of the *T. pantotropha* oxidized cytochrome cd_1. Such assignments are strictly valid only when taken together with the EPR spectra, measurable only at low temperatures. However, these assignments *are* consistent with the EPR spectra presented below. There is also a significant derivative shaped band in Figure 4c, in the 800−1200 nm region. By analogy with the properties of protohemes (*42*−*44*), we assign this as the NIR-CT band of the *high-spin* ferric heme d_1 population, which is present at room temperature in the *T. pantotropha* enzyme.

Table 1: EPR *g*-Values and Heme d_1 α-Band Wavelength Maxima for Cytochromes cd_1

	heme *c* ($g_{z,y,x}$)	heme d_1 ($g_{x,y,z}$)	λ_{LS}[a] (nm)	λ_{HS}[b] (nm)	refs
Thiosphaera pantotropha	3.05, −, −	2.52, 2.19, 1.84	644	702	this work
Pseudomonas stutzeri (ZoBell)	2.97, 2.24, ∼1.4	2.56, 2.42, 1.58	641		this work
Thiobacillus denitrificans	3.60, −, −	2.50, 2.43, 1.70	642		35, 46
Pseudomonas aeruginosa	2.97, 2.26, 1.40	2.51, 2.42, 1.73	640		12, 18, 38, 47
Pseudomonas nautica 617			636		48
Paracoccus halodenitrificans			636		49
Ralstonia (formerly *Alcaligenes*) *eutropha*			∼640		17
Magnetospirillum magnetotacticum			643		50
Roseobacter denitrificans, form 1			∼640	700	51
Roseobacter denitrificans, form 2			640		51

[a] The wavelength maxima of the α-bands assigned to the low-spin ferric forms of heme *d*. [b] The wavelength maxima of the α-bands assigned to the high-spin ferric forms of heme d_1.

In Figure 4b, an extremely weak positive band is observed between 1900 and 2500 nm. The CT band for low-spin ferric protohemes is seen at such long wavelengths only for bis-methionine coordination (*19*, *45*). The EPR spectrum (below) contains no signals that are characteristic of this coordination, and the 2170 nm band is assigned as the porphyrin (π)-to-Fe(II) (d) CT transition of the low-spin ferric heme d_1. In the *T. pantotropha* spectra of Figure 4, panels c and d, a weak band is observed to higher energy than this in the 1650−1900 nm region. The possibility that this is also a heme d_1 CT band is discussed below. This band is observed at both 4.2 K and RT, whereas the 2170 nm band for the *P. stutzeri* enzyme was not detected at room temperature. However, the heme d_1 CT band is substantially weaker at RT compared to 4.2 K, and spectrometer sensitivity is reduced at wavelengths >2000 nm. It cannot therefore be ruled out that the 2170 nm band is present at higher temperatures. Indeed, it is likely to be present as the UVV MCD show heme d_1 to be low-spin at all temperatures for the *P. stutzeri* enzyme.

Note that the estimated intensity of a *T. pantotropha* heme d_1 CT band is therefore ∼4 M^{-1} cm^{-1} and, at the enzyme concentrations used, this is close to the instrumental detection limit.

EPR Spectra. The X-band EPR spectra at 10 K of both cytochromes cd_1 are presented in Figure 5. The spectrum of the *P. stutzeri* enzyme (Figure 5a) is similar to that reported for cd_1 from *P. aeruginosa*. The assignments of features to each of the two hemes for these and other cytochromes cd_1 are collected in Table 1. The three *P. stutzeri* features at $g = 2.97$, 2.24, and 1.4 constitute a typical spectrum seen for many low-spin ferric protohemes where the orientation of axial ligands results in high *rhombicity* at the ferric ion. This is assigned to low-spin ferric heme *c*. The signal at $g = 1.58$ is unlikely to be the third *g*-value of this heme, as this would result in $\sum g^2 = 16.3$. It is known that, for such a spectrum, the sum of the squares of the *g* values does not exceed 16 (*52*). The $g = 1.4$ feature is similarly broad and difficult to detect for the *P. aeruginosa* enzyme.

This spectrum is an example of one of the two limiting types of EPR behavior encountered for low-spin ferric protohemes. When axial ligand orientation promotes π-bonding of very different magnitudes in the *x* and *y* directions of the heme plane, then a "rhombic" type spectrum results (*53*). As for heme *c* in the *P. stutzeri* and *P. aeruginosa* enzymes, all three *g*-values can usually be detected (Table 1).

Heme *c* of *T. pantotropha* cd_1 gives rise to the second category of EPR, a "large g_{max}" type spectrum where g_z is >3 and the other two *g* values are not easily detected. This form of spectrum is frequently encountered for hemes bound to two histidines with ligand planes oriented closer to perpendicular than to parallel (*53*). This is the case for heme *c* in the three-dimensional structure of the *T. pantotropha* oxidized enzyme where the angle is ∼60° (*11*). However, in certain cases, large g_{max} spectra can arise for hemes with histidine-methionine coordination (*28*, *54*). The $g = 3.05$ signal (*T. pantotropha*) is assigned as the g_z-value for heme *c*.

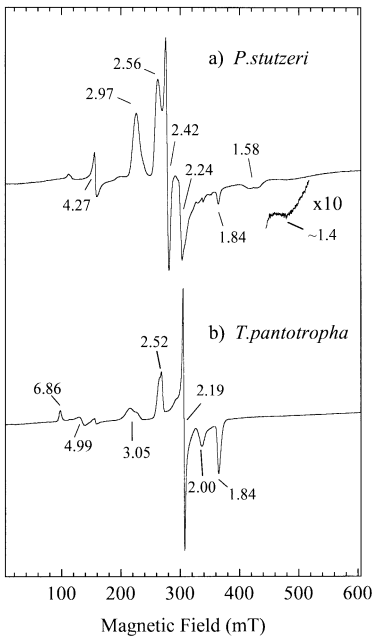

FIGURE 5: X-band EPR spectra of oxidized cytochromes cd_1. (a) *P. stutzeri* cd_1 (1.13 mM); (b) *T. pantotropha* cd_1 (490 μM). Both spectra were recorded at 10 K using 2.02 mW incident microwave power and 1 mT modulation amplitude. Buffers were as described in Materials and Methods.

The EPR features at $g = 2.56$, 2.42, and 1.58 (*P. stutzeri*) and $g = 2.52$, 2.19, and 1.84 (*T. pantotropha*) are assigned to the enzymes' respective low-spin ferric hemes d_1. These spectra have unusually low values of $\sum g^2 = 14.9$ and 14.5 which are characteristic of low-spin ferric hydroporphyrins but not generally found for protohemes. These differences also influence the MCD spectra and may have important consequences for the properties of heme d_1, which are discussed below. Features at $g = 6.86$ and 4.99 in the spectrum for *T. pantotropha* are characteristic of rhombically distorted high-spin ferric heme and may represent a trace of high-spin heme d_1. The feature at $g = 4.27$ for *P. stutzeri* is from adventitiously bound ferric ion.

One other observation warrants comment. Both spectra show trace features at *g* values characteristic of one of the major heme signals in the other spectrum. Thus, in the *T. pantotropha* spectrum, the low-field *g*-value of each heme ($g = 3.05$ and 2.52) displays a minor shoulder near one of the *g* values for the equivalent heme in the *P. stutzeri* spectrum. Similarly, *P. stutzeri* cd_1 shows a minority feature at $g = 1.84$.

DISCUSSION

Heme c. This work shows that heme *c* of *P. stutzeri* cd_1 has histidine-methionine ligation, as was observed for the enzyme of *P. aeruginosa* (*18*). These results from the two *Pseudomonas* proteins in solution contrast markedly with the observation that, in the three-dimensional structure of *T. pantotropha* oxidized cd_1, heme *c* has bis-histidine ligation. The MCD data therefore provide important confirmation that heme *c* of oxidized *T. pantotropha* cd_1 *in solution* has two histidine ligands as it does in the crystalline state. It appears then that the ligation at heme *c* defines two distinct classes of *oxidized* cytochrome cd_1. Although the EPR spectrum of heme *c* for *T. pantotropha* is clearly different to those seen for *P. stutzeri* and *P. aeruginosa*, this alone is not a reliable indicator of ligation and it requires knowledge of the NIR MCD spectrum to unambiguously identify changes in heme ligands. The EPR spectrum is sensitive to ligand *orientation* whereas changes in the wavelength of the MCD NIR-CT report on ligand *identity*.

EPR data have also been reported for the cd_1 from *T. denitrificans*. Heme *c* gives rise to a single feature at $g = 3.6$ and it has been suggested that this is due to bis-histidine ligation (*55*). However, this assignment needs verification. If true, then the *T. denitrificans* cd_1 would appear to combine the heme *c* EPR properties of the *T. pantotropha* enzyme with the heme d_1 optical and EPR properties of the two *Pseudomonas* enzymes (*vide infra*).

Heme d. The optical spectra reported here for *T. pantotropha* cd_1 reveal that the heme d_1 is in a thermal spin-state equilibrium, between high- and low-spin forms, over the temperature range 1.75−300 K. Two explanations for this can be considered. First, it is possible that the field generated by the ligands tyrosinate, histidine, and the d_1 hydroporphyrin places the Fe(III) ion close to the thermal spin-crossover with the low-spin Fe(III) state being lower in energy. The alternative is that, at room temperature, a percentage of heme d_1 is lacking one axial ligand possibly tyrosinate, so that the heme exists both as a six- and a five-coordinate species with the ligand rebinding on cooling. However, the RT absorption spectrum shows a significant proportion of the two species, implying that a high percentage of the d_1 would be in the ligand off state. This is not consistent with crystallographic data which show the invariance of heme d_1 iron ligation in crystals at room and cryogenic temperatures (*13*). This shows unequivocally that the histidine/tyrosine ligands to heme d_1 in *T. pantotropha* cd_1 both remain bound in the form giving rise to the split α-absorption. Substantial rearrangement in the coordination sphere of the ferric ion are also unlikely to occur in frozen solution at temperatures down to 1.75 K. Hence, we favor the former explanation.

The heme d_1 of *T. pantotropha* cytochrome cd_1 is thus far unique in its ligation state of His-Tyr, although there are well-authenticated examles of Tyr/His ligation for protohemes. The H64Y mutants of sperm whale and horse heart myoglobins both contain Tyr/His ligated hemes with iron-ligand bond lengths (Tyr/His) of 1.92/2.58 and 2.24/2.26 Å respectively (*56*). Fe(III), therefore, is strictly six coordinate. However, the Fe(III) ion is high spin both at RT and at 4.2 K in this mutation. In contrast, the F43Y mutant of human myoglobin has heme MCD properties, which show that although it too has a heme with Tyr/His coordination it exists in a temperature-dependent spin mixture (Seward, H., Cheesman, M. R., and Thomson, A. J., unpublished data). We clearly need to understand further the subtleties of tyrosinate ligation to Fe(III) heme and the factors which determine whether or not the system is placed close to the spin-crossover. The changes required to move these systems onto or away from the spin-crossover are small compared to those required to shift optical bands significantly. Thus, the Tyr/His ligated protohemes have variable spin properties, but all give rise to high-spin ferric CT bands at similar wavelengths, wavelengths which also show that tyrosinate has a ligand field strength similar to that of hydroxide ion [Seward, H., Cheesman, M. R., and Thomson, A. J., unpublished data]. The absorption spectra of crystals of *T. pantotropha* cd_1 show absorption bands at ∼646 and ∼704 nm with the same temperature-dependent behavior observed for the solution spectra (*57*). This shows unequivocally that the ligand state of heme d_1 is unaltered between the crystal and solution phases.

Although heme d_1 in oxidized *T. pantotropha* cd_1 exists in a spin equilibrium while its counterpart in *P. stutzeri* cd_1 is pure low spin, this is not necessarily due to different heme d_1 ligation in the two enzymes. Indeed, the evidence from electronic absorption data on heme d_1 is to the contrary. When treated with imidazole, heme d_1-substituted myoglobin and cytochrome cd_1 give ferric heme d_1 α-bands close in energy at 627 and 631 nm, respectively. bis-Imidazole heme d_1 has an α-absorption at 625 nm. Thus, in a variety of proteins it is clear that the same heme d_1 ligation results in α-bands within a narrow wavelength region. Substitution of cyanide ion for one imidazole or histidine ligand in these species causes a shift to the red of ∼3 nm (*37*, *58*), suggesting that the α-band is sensitive to ligand substitution. However, the low-spin ferric heme d_1 α-bands reported here for the two enzymes are close together at 641 (*P. stutzeri*) and 644 nm (*T. pantotropha*), a shift to the red of >10 nm for the wavelengths anticipated for bis-histidine ligation at heme d_1. Indeed, all heme d_1 α-bands reported for oxidized cytochromes cd_1 lie in the wavelength range 636−644 nm (Table 1). This includes the *low-spin* α-band for the only two reported cytochromes cd_1 with *two* bands, namely the *T. pantotropha* enzyme examined here and one of two forms of cytochrome cd_1 isolated from the closely related species *Roseobacter denitrificans* (formerly *Erythrobacter*) (*51*). The form with two heme d_1 α-bands also has a shoulder near 430 nm, as seen for *T. pantotropha* cd_1. Thus, the low-spin heme d_1 α-band occurs at similar wavelengths in all cytochromes cd_1, showing that in all these enzymes heme d_1 experiences an axial ligand field comparable in strength to that found for *T. pantotropha*. This suggests that all have His/Tyr, or possibly His/hydroxide, ligation. But if it is reasonably assumed that the totally conserved histidine (His-200 in *T. pantotropha*) is the common heme d_1 proximal ligand, then the conserved histidine, lysine, and methionine

Table 2: Ground State Parameters of Heme d_1 Derived from Analysis of the EPR *g*-Values[a]

	g_x	g_y	g_z	tetragonality Δ/λ	rhombicity V/Δ	*a* (d_{yz})	*b* (d_{zx})	*c* (d_{xy})
Thiosphaera pantotropha	1.84	2.19	2.52	5.79	3.61	0.98	0.14	0.07
	−2.52	2.19	−1.84	−5.60	−3.98	0.07	0.14	0.98
Pseudomonas stutzeri (ZoBell)	−2.42	2.56	−1.58	−3.08	0.58	0.19	0.16	0.96
Thiobacillus denitrificans	−2.43	2.50	−1.70	−3.58	0.39	0.16	0.14	0.97
Pseudomonas aeruginosa	−2.43	2.51	−1.71	−3.61	0.45	0.16	0.14	0.97

[a] Parameters are defined and calculated as described in ref 58 and illustrated in Figure 6.

residues (Figure 1), all potential heme ligands, are ruled out as candidates for the distal position. If other cytochromes cd_1 do have distal heme d_1 tyrosinate ligands, then it is intriguing that only *P. aeruginosa* possesses a candidate residue near the N-terminus. Otherwise, the sequences shown in Figure 1 suggest two possible residues. All sequences have a conserved tyrosine at position 61 but we note also that all but one have tyrosine at residue 100 (*T. pantotropha* numbering). Paradoxically, this would imply that the *T. pantotropha* enzyme has the same heme d_1 ligand set but not by making use of one of the conserved tyrosine residues.

MCD studies of *P. aeruginosa* oxidized cd_1 showed that the *c*-type cytochrome has His-Met coordination, but no NIR-CT bands from heme d_1 could be detected. We show here for *the first time* that heme d_1 does give rise to a CT band in the NIR region of comparable intensity to those of ferric chlorin systems. The observation of this band by MCD provides valuable information on the electronic ground state of heme d_1, which is discussed below, but does not yet assist with the identification of the ligands in the *P. stutzeri* enzyme. Before this approach can be used successfully, the weak NIR-CT band must be located first for a series of well understood heme d_1 model compounds and then for cytochromes cd_1 other than that from *P. stutzeri*. It then remains to be seen whether or not variations in the energy of these bands do contain information concerning heme ligation in the way the equivalent transitions for low-spin ferric protohemes have proved so useful (*19*, *20*).

The assignment of axial ligands using the energy of the NIR-CT band in the MCD is a well-established method for low-spin ferric protohemes. For calibration, the approach relies on MCD data for low-spin ferric photohemes whose axial ligands are already known from other methods. There is no equivalent body of data for ferric hydroporphyrins. Some NIR MCD data is available for low-spin ferric derivatives of HPII and of heme *d* substituted myoglobins (*23*, *25*, *27*). Weak CT bands are observed to vary in energy for nine different modes of axial ligation. While this is a very limited data set, it is notable that the energies of the bands are all approximately 3500 cm^{-1} shifted to lower energy compared to those of protohemes with the same ligands.

Electronic Ground State of Heme d_1. Taken together, the MCD and EPR properties establish that the low-spin ferric form of heme d_1 is an example of a $(d_{xz},d_{yz})^4(d_{xy})^1$ ground state and thus places it, along with low-spin ferric heme *d*, in a subclass distinct from low-spin ferric protohemes. In any low-spin ferric heme, the unpaired electron is distributed among the t_{2g} set of three d-orbitals, i.e., within d_{yz}, d_{zx}, and d_{xy}. The order and separation of the 1-electron energies of these orbitals (Figure 6) will determine the exact distribution within the set. The t_{2g} orbital set in octahedral symmetry

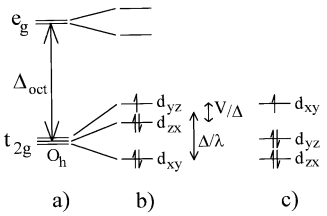

FIGURE 6: Energy level schemes for iron d-orbitals in low-spin ferric hemes, as described in text.

(Figure 6a) is further split by tetragonal and rhombic distortions caused largely by the axial ligands (Figure 6b). These distortions are described (*59*) by the parameters Δ/λ and V/Δ, respectively. The unpaired spin distribution can be described by a wavefunction expressed in terms of the coefficients *a*, *b*, and *c*, which represent the contribution to the wavefunction from each of the t_{2g} orbitals. The coefficients and the distortion parameters can all be calculated directly from the EPR *g*-values (*52*, *59*, *60*). This has been done for known heme d_1 EPR features and the results are given in Table 2. The d-orbital energy ordering illustrated in Figure 6b is that encountered for normal low-spin ferric hemes where the unpaired spin is found largely within the d_{zx},d_{yz} pair. The spin distributions deduced from the *g*-values and tabulated for hemes d_1 are shown in the final three columns of Table 2. They show that, for these hemes, the spin is predominantly localized in the d_{xy} orbital, a consequence of the stabilization of the d_{zx},d_{yz} pair relative to d_{xy}. This situation is described by a *negative* tetragonality parameter Δ/λ (Figure 6c). Note that the set $g = 2.52$, 2.19, and 1.84 for heme d_1 of *T. pantotropha* cd_1 gives two possible solutions, the first of which represents the usual $(d_{xy})^2(d_{xz}d_{yz})^3$ protoheme ground state, but this can be discounted on the basis of the weak NIR MCD spectra (*29*). The table shows that heme d_1 in all four species reported has an unusual ferric electronic ground states in which the unpaired spin is largely in an orbital located in the plane of the isobacteriochlorin macrocycle rather than in orbitals which extend above the macrocyclic plane as is the case for low-spin ferric protohemes. The experimental criteria for this state have been established by Walker and co-workers over a number of years, and recently, the properties of the EPR spectra and the nature of the NIR-CT bands expected from the ground state $(d_{xz}d_{yz})^4(d_{xy})^1$ have been reported (*29*). The EPR *g*-values are a rhombic trio with unusually low *g*-value anisotropy, since the unpaired electron in the d_{xy} orbital has a reduced orbital moment. The porphyrin-to-Fe(III) CT transitions, from $\pi(a_{1u},a_{2u})$ to d_{xy}, are formally forbidden and hence very weak [$\Delta\epsilon \leq 60$ M^{-1} cm^{-1} for low-spin ferric chlorins compared to 130−600 M^{-1} cm^{-1} for protohemes (*19*, *20*, *23*, *25*, *27*)]. These properties are found in the EPR and MCD spectra of heme d_1, and so we are able to assign the weak MCD bands at 2170 nm (*P. stutzeri*) as the NIR-CT band for the heme d_1.

One question posed by these findings is what are the chemical properties of a $(d_{xy})^1$ ground state of Fe(III) low-spin hemes compared with those of a more typical $(d_{xy},d_{yz})^3$ ground state? This is unknown but it is likely that the unusual unpaired spin distribution plays an important role. In the case of $(d_{xy})^1$, an unpaired electron is placed in an orbital which lies in the plane of the porphyrin ring, whereas for the $(d_{xy,yz})^3$ state the unpaired electron is in orbitals which can π-bond with axial ligands such as O_2 and NO. Thus, Fe(III) $(d_{xy})^1$ is a stronger π-donor and a weaker π-acceptor. This may weaken the binding strength between Fe(III) and NO, for example, and assist in the loss of NO from heme d_1 at the end of the catalytic cycle (*11*). The factors which generate a $(d_{xy})^1$ ground state are a strong axial ligand field relative to the in-plane field of the porphyrin ring. There are few ligands available in proteins capable of generating such a powerful axial field, although the thiolate side chain of cysteine may be an example. The alternative is therefore to weaken the in-plane field relative to the axial field. Partial saturation of the porphyrin ring, as in heme d_1, may accomplish this. Other examples in biology of porphyrin rings which seem to bring about $(d_{xy})^1$ ground states are heme *d* in *Escherichia coli* HP II and in siroheme, both cases in which the porphyrin ring is partially saturated.

Ligand Assignments. The combined evidence from the spectroscopic work presented in this paper shows that heme *c* in nitrite reductase from the species *P. stutzeri* and *T. pantotropha* has different ligation states in the resting, oxidized form of the enzymes. There were already indications in the literature that this would turn out to be the case. Sequence alignments when combined with the crystal structure of the *T. pantotropha* oxidized cd_1 show that the His-17 ligand of the heme *c* is not conserved in the sequences of several other cytochromes cd_1 (Figure 1). However, it is now known that, on reduction of crystalline *T. pantotropha* enzyme, a ligand switch occurs at heme *c* to give histidine-methionine coordination (*61*). His-17 is replaced by Met-106, one of two totally conserved methionines (Figure 1). It is likely then that the equivalent methionine in the sequences of the *P. stutzeri* and *P. aeruginosa* enzymes is already a heme *c* ligand in the oxidized state. A shoulder at $g \approx 2.97$ noted in the EPR spectrum of the *T. pantotropha* enzyme (Figure 5) suggests that a minor amount of heme *c* actually has histidine-methionine coordination in the solution sample. This proposition finds some support in the NIR MCD of Figure 4. For both MCD and electronic absorption, the intensity of the NIR-CT band is governed by the orbital coefficients *a* and *b* (Table 1) because a transition from the porphyrin $\pi(a_{1u},a_{2u})$ orbitals to the ferric d_{xy}-orbital is formally forbidden. The expression for the MCD intensity includes the term $g_z ab$ (*62*, *29*). Using this to estimate the relative intensities of the heme d_1 CT MCD bands yields the value of 0.38 for the ratio of a *T. pantotropha* band to that for *P. stutzeri*. In contrast, in Figure 4, it appears to be larger with a ratio of 3.7. This casts doubt on the 1650−1900 nm feature being the *T. pantotropha* heme d_1 CT band. It may actually be all or partially due to a proportion of the heme *c* with histidine-methionine coordination. It is clear, however, that this is not due to partial reduction of the enzyme. Although diamagnetic, reduced low-spin ferrous hemes give exceptionally sharp intense visible region MCD signals and would be easily observed at levels of a few percent in the spectra of Figure 3 (*19*).

CONCLUSIONS

The spectroscopic results presented here make clear that the heme ligation states revealed by the crystal structure of *T. pantotropha* oxidized cytochrome cd_1 are unchanged in the solution form of this enzyme. However, since only one of the ligands to each heme is conserved in known sequences, this therefore raises the question of the relevance of this form to the catalytic pathway assuming that all cytochromes cd_1 function by the same reaction mechanism. It is possible that the *T. pantotropha* cd_1 structure represents a resting form of the enzyme. This particular view is given some credence by the knowledge that, upon reduction of the enzyme, heme *c* switches ligands to His/Met and heme d_1 loses the tyrosinate ligand (*61*). The *Pseudomonas* enzymes have His/Met ligated heme *c* in the oxidized state, and heme d_1 is known to go high-spin when reduced (*12*). So it can be proposed that, following reduction, all cytochromes cd_1 will have similar heme ligation prior to binding substrate. It needs to be determined whether or not they all cycle through equivalent oxidized states. If they do then the known structure of the *T. pantotropha* enzyme may represent some form of resting state. Alternatively, there may be a real difference in the mechanisms of cytochromes cd_1 isolated from different bacteria and the ligand switching at the c-heme together with tyrosine displacement and religation at the d_1 heme may provide a catalytic advantage, the nature of which will have to be established by future work.

The identification of heme d_1 as having an unusual ground state in the low-spin Fe(III) state may have relevance to turnover if the binding affinity of the product, NO, is reduced. This may be a mechanism for facilitating release of product from the enzyme, followed by rebinding of tyrosinate or hydroxide ion.

ACKNOWLEDGMENT

A.J.T. and M.R.C. would like to thank Dr. P. M. A. Gadsby and Hitachi Scientific Instruments for providing the U-4001 accessory allowing the measurement of ultra-low-temperature absorption spectra. MRC would like to thank Dr. Ben Berks for helpful discussions. Pamela Williams, Vilmos Fülöp, and Janos Hadju are thanked for discussing the *T. pantotropha* cytochrome cd_1 structure and the spectra of the crystals with us.

NOTE ADDED IN PROOF

The structure of the cytochrome cd_1 from *Pseudomonas aeruginosa* has now been solved [Nurizzo, D., Silvestrini, M.-C., Mathieu, M., Cutruzzolà, F., Bourgeois, D., Fülöp, V., Hajdu, J., Brunori, M., Tegoni, M., and Cambillau, C. (1997) *Structure 5*, 1157−1171] and confirms the histidine-methionine coordination at heme *c*. The ligands to heme d_1 are histidine and hydroxide ion.

REFERENCES

1. Payne, W. J. (1973) *Bacterial. Rev. 37*, 409−452.
2. Zumft, W. G. (1993) *Arch. Microbiol. 160*, 253−264.
3. Berks, B. C., Ferguson, S. J., Moir, J. W. B., and Richardson, D. J. (1995) *Biochim. Biophys. Acta 1232*, 97−173.
4. Godden, J. W., Turley, S., Teller, D. C., Adman, E. T., Liu, M. Y., Payne, W. J., and Legall, J. (1991) *Science 253*, 438−442.

5. Kukimoto, M., Nishiyama, M., Murphy, M. E. P., Turley, S., Adman, E. T., Horinouchi, S., and Beppu, T. (1994) *Biochemistry 33*, 5246−5252.
6. Chang, C. K. (1985) *J. Biol. Chem. 260*, 9520−9522.
7. Chang, C. K., and Wu, W. (1986) *J. Biol. Chem. 261*, 8593−8596.
8. Silvestrini, M. C., Tordi, M. G., Musci, G., and Brunori, M. (1990) *J. Biol. Chem. 265*, 11783−11787.
9. Horio, T., Higashi, T., Yamanaka, T., Matsubara, H., and Okunuki, K. (1961) *J. Biol. Chem. 236*, 944−951.
10. Fülöp, V., Moir, J. W. B., Ferguson, S. J., and Hajdu, J. (1993) *J. Mol. Biol. 232*, 1211−1212.
11. Fülöp, V., Moir, J. W. B., Ferguson, S. J., and Hajdu, J. (1995) *Cell 81*, 369−377.
12. Walsh, T. A., Johnson, M. K., Greenwood, C., Barber, D., Springall, J. P., and Thomson, A. J. (1979) *Biochem. J. 177*, 29−39.
13. Baker, S. C., Saunders, N. F. W., Willis, A. C., Ferguson, S. J., Hajdu, J., and Fülöp, V. (1997) *J. Mol. Biol. 269*, 440−455.
14. Silvestrini, M. C., Galeotti, C. L., Gervais, M., Schinina, E., Barra, D., Bossa, F., and Brunori, M. (1989) *FEBS Lett. 254*, 33−38.
15. Jüngst, A., Wakabayashi, S., Matsubara, H., and Zumft, W. G. (1991) *FEBS Lett. 279*, 205−209.
16. Weeg-Aerssens, E., Wu, W., Ye, R. W., Tiedje, J. M., and Chang, C. K. (1991) *J. Biol. Chem. 266*, 7496−7502.
17. Sann, R., Kostka, S., and Friedrich, B. (1994) *Arch. Microbiol. 161*, 453−459.
18. Sutherland, J., Greenwood, C., Peterson, J., and Thomson, A. J. (1986) *Biochem. J. 233*, 893−898.
19. Cheesman, M. R., Greenwood, C., and Thomson, A. J. (1991) *Adv. Inorg. Chem. 36*, 201−255.
20. Gadsby, P. M. A., and Thomson, A. J. (1990) *J. Am. Chem. Soc. 112*, 5003−5011.
21. Keegan, J. D., Stolzenberg, A. M., Lu, Y-C., Linder, R. E., Barth, G., Bunnenberg, E., and Djerassi, C. (1981) *J. Am. Chem. Soc. 103*, 3201−3203.
22. Dawson, J. H., Bracete, A. M., Huff, A. M., Kadkhodayan, S., Zeitler, C. M., Sono, M., Chang, C. K., and Loewen, P. C. (1991) *FEBS Lett. 295*, 123−126.
23. Peng, Q., Timkovitch, R., Loewen, P. C., and Peterson, J. (1992) *FEBS Lett. 309*, 157−160.
24. Huff, A. M., Chang, C. K., Cooper, D. K., Smith, K.M., and Dawson, J. H. (1993) *Inorg. Chem. 32*, 1460−1466.
25. Peng, Q., and Peterson, J. (1994) *FEBS Lett. 356*, 159−161.
26. Bracete, A. M., Kadkhodayan, S., Sono, M., Huff, A. M., Zhuang, C., Cooper, D. K., Smith, K. M., Chang, C. K., and Dawson, J. H. (1994) *Inorg. Chem. 33*, 5042−5049.
27. Peng, Q. (1994) Ph.D. Thesis, University of Alabama.
28. Spinner, F., Cheesman, M. R., Thomson, A. J., Kaysser, T., Gennis, R. B., Peng, Q., and Peterson, J. (1995) *Biochem. J. 308*, 641−644.
29. Cheesman, M. R., and Walker, F. A. (1996) *J. Am. Chem. Soc. 118*, 7373−7380.
30. Coyle, C. L., Zumft, W. G., Kroneck, P. M. H., Körner, H., and Jakob, W. (1985) *Eur. J. Biochem. 153*, 459−467.
31. Moir, J. W. B., Baratta, D., Richardson, D. J., and Ferguson, S. J. (1993) *Eur. J. Biochem. 212*, 377−385.
32. Thomson, A. J., Cheesman, M. R., and George, S. J. (1993) *Methods Enzymol. 226*, 199−232.
33. Stolzenberg, A. M., Strauss, S. H., and Holm, R. H. (1981) *J. Am. Chem. Soc. 103*, 4763−4778.
34. Walsh, T. A., Johnson, M. K., Barber, D., Thomson, A. J., and Greenwood, C. (1980) *J. Inorg. Biochem. 14*, 15−31.
35. Huynh, B. H., Lui, M. C., Mouras, J. J. G., Moura, I., Ljungdahl, P. O., Münck, E., Payne, W. J., Peck, H. D. Jr., DerVartanian, D. V., and LeGall, J. (1982) *J. Biol. Chem. 257*, 9576−9581.
36. Vickery, L. E., Palmer, G., and Wharton, D. C. (1978) *Biochem. Biophys. Res. Commun. 80*, 458−463.
37. Steup, M. B., and Muhoberac, B. B. (1989) *J. Inorg. Biochem. 37*, 233−258.
38. Muhoberac, B. B., and Wharton, D. C. (1983) *J. Biol. Chem. 258*, 3019−3027.
39. Yamanaka, T., and Okunuki, K. (1963) *Biochim. Biophys. Acta 67*, 379−393.
40. Piepho, S. B., and Schatz, P. N. (1980) *Group Theory in Spectroscopy, with Applications to Magnetic Circular Dichroism*, Wiley, New York.
41. Stephens, P. J. (1976) *Adv. Chem. Phys. 35*, 197−246.
42. Brill, A. S., and Williams, R. J. P. (1961) *Biochem. J. 78*, 246−253.
43. Braterman, P. S., Davies, R. C., and Williams, R. J. P. (1964) *Adv. Chem. Phys. 7*, 359−407.
44. Cheng, J. C., Osborne, G. A., Stephens, P. J., and Eaton, W. A. (1973) *Nature (London) 241*, 193−194.
45. Barker, P. D., Nerou, E. P., Cheesman, M. R., Thomson, A. J., de Oliveira, P., and Hill, H. A. O. *(1996) Biochemistry 35*, 13618−13626.
46. LeGall, J., Payne, W. J., Morgan, T. V., and DerVartanian, D. (1979) *Biochem. Biophys. Res. Commun. 87*, 355−362.
47. Gudat, J. C., Singh, J., and Wharton, D. C. (1973) *Biochim. Biophys. Acta 292*, 376−390.
48. Besson, S., Carneiro, C., Moura, J. J. G., Moura, I., and Fauque, G. (1995) *Anaerobe 1*, 219−226.
49. Mancinelli, R. L., Cronin, S., and Hochstein, L. I. (1986) *Arch. Microbiol. 145*, 202−208.
50. Yamazaki, T., Oyanagi, H., Fujiwara, T., and Fukumori, Y. (1995) *Eur. J. Biochem. 233*, 665−671.
51. Doi, M., Shioi, Y., Morita, M., and Takamiya, K. (1989) *Eur. J. Biochem. 184*, 521−527.
52. Bohan, T. L. (1997) *J. Magn. Reson. 26*, 109−118.
53. Walker, F. A., Huynh, B. H., Scheidt, W. R., and Osvath, S. R. (1986) *J. Am. Chem. Soc. 108*, 5288−5297.
54. Gadsby, P. M. A., Hartshorn, R. T., Moura, J. J. G., Sinclair-Day, J. D. Sykes, A. G., and Thomson, A. J. (1989) *Biochim. Biophys. Acta 994*, 37−46.
55. Huynh, B. H. (1994) *Methods Enzymol. 243*, 523−543.
56. Hargrove, M. S., Singleton, E. W., Quillin, M. L., Ortiz, L. A., Phillips, G. N., Jr., Mathews, A. J., and Olson, J. S. (1994) *J. Biol. Chem. 269*, 4207−4214.
57. Williams, P. A. (1997) Ph.D. Thesis, University of Oxford.
58. Walsh, T. A., Johnson, M. K., Thomson, A. J., Barber, D., and Greenwood, C. (1981) *J. Inorg. Biochem. 14*, 1−14.
59. Taylor, C. P. S. (1977) *Biochim. Biophys. Acta 491*, 137−149.
60. Griffith, J. S. (1971) *Mol. Phys. 21*, 135−139.
61. Williams, P. A., Fülöp, V., Garman, E. F., Saunders, N. F. W., Ferguson, S. J., and Hajdu, J. (1997) *Nature 389*, 406−412.
62. Thomson, A. J., and Gadsby, P. M. A. (1990) *J. Chem. Soc., Dalton Trans.* 1921−1928.

BI971677A